

Article

Cost-Effective and Portable Instrumentation to Enable Accurate pH Measurements for Global *Industry 4.0* and *Vertical Farming* Applications

Rolando Hinojosa-Meza ¹, Ernesto Olvera-Gonzalez ^{1,*}, Nivia Escalante-Garcia ¹, José Alonso Dena-Aguilar ², Martín Montes Rivera ³ and Paulino Vacas-Jacques ^{1,2,*}

¹ Laboratorio de Iluminación Artificial, Tecnológico Nacional de México/IT de Pabellón de Arteaga, Carretera a la Estación de Rincón Km. 1, Aguascalientes 20670, Mexico; rolando.hm@pabellon.tecnm.mx (R.H.-M.); nivia.eg@pabellon.tecnm.mx (N.E.-G.)

² Departamento de Ingenierías, Tecnológico Nacional de México/IT de Pabellón de Arteaga, Carretera a la Estación de Rincón Km. 1, Aguascalientes 20670, Mexico; jose.da@pabellon.tecnm.mx

³ Dirección de Posgrados e Investigación, Universidad Politécnica de Aguascalientes, Calle Paseo San Gerardo #201, Fracc. San Gerardo, Aguascalientes 20342, Mexico; martin.montes@upa.edu.mx

* Correspondence: jose.og@pabellon.tecnm.mx (E.O.-G.); paulino.vj@pabellon.tecnm.mx (P.V.-J.)

Abstract: Global *Vertical Farming* (VF) applications with characteristic *Industry 4.0* connectivity will become more and more relevant as the challenges of food supply continue to increase worldwide. In this work, a cost-effective and portable instrument that enables accurate pH measurements for VF applications is presented. We demonstrate that by performing a well-designed calibration of the sensor, a near Nernstian response, 57.56 [mV/pH], ensues. The system is compared to a ten-fold more expensive laboratory gold standard, and is shown to be accurate in determining the pH of substances in the 2–14 range. The instrument yields precise pH results with an average absolute deviation of 0.06 pH units and a standard deviation of 0.03 pH units. The performance of the instrument is ADC-limited, with a minimum detectable value of 0.028 pH units, and a typical absolute accuracy of ± 0.062 pH units. By meticulously designing bias and amplification circuitry of the signal conditioning stage, and by optimizing the signal acquisition section of the instrument, a (minimum) four-fold improvement in performance is expected.

Keywords: pH-instrument; *Vertical Farming*; *Industry 4.0*; Nernstian response; cost-effective; portable; instrumentation



Citation: Hinojosa-Meza, R.; Olvera-Gonzalez, E.; Escalante-Garcia, N.; Dena-Aguilar, J.A.; Montes Rivera, M.; Vacas-Jacques, P. Cost-Effective and Portable Instrumentation to Enable Accurate pH Measurements for Global *Industry 4.0* and *Vertical Farming* Applications. *Appl. Sci.* **2022**, *12*, 7038. <https://doi.org/10.3390/app12147038>

Academic Editor: Amy J. C. Trappey

Received: 11 June 2022

Accepted: 5 July 2022

Published: 12 July 2022

Publisher's Note: MDPI stays neutral with regard to jurisdictional claims in published maps and institutional affiliations.



Copyright: © 2022 by the authors. Licensee MDPI, Basel, Switzerland. This article is an open access article distributed under the terms and conditions of the Creative Commons Attribution (CC BY) license (<https://creativecommons.org/licenses/by/4.0/>).

1. Introduction

Globally, numerous industries employ the pH level for multiple purposes. For instance, the pH is recurrently used as a central metric to determine the alkalinity. Furthermore, by controlling the pH, an efficient coagulation of sludge in wastewater can be guaranteed [1–3]. Similarly, pH serves as a reference to monitor and prevent corrosion in pipes and boilers [4,5]. In fermentation processes, continuous quantification of the pH is relevant to avoid the generation of unwanted and harmful by-products [6–8]. In the brewing industry, the pH serves to determine aging, increments in hop hardness, and bittering concentrations [9–11]. For perishable products, such as meat and fish, the pH level reveals shelf life and freshness [12–15]. Finally, the pH is central to determine ripening stage, as a function of ethylene concentration, of fruits and vegetables [16–18].

Our laboratory specializes in applied research and technology development in the field of *Precision Farming* (PF). PF is defined as the optimal utilization of technology to accurately assess: planting density, fertilizer quantity, and farming supplies, as needed to precisely predict crop production and yield [19].

Of particular interest to our group is the important field of *Vertical Farming* (VF). VF refers to systems of agriculture where salads, microgreens, herbs, etc. are grown

under artificial light as supplemental irradiation, and sensing technology is integrated to continuously improve quality and yield. VF ensures sustainability by addressing the problem of food security for the growing population around the world [20]. In VF solutions, plants are produced in *Closed Plant Production Systems*, which are generally hydroponic, aeroponic, or aquaponic [21]. In particular, a VF hydroponic system is being constructed in our laboratory, which consists of three distinct vertical racks where various plants can be grown. Each variety is exposed to a specific light recipe depending on the plant characteristics. Ambient humidity and temperature sensors are distributed along the racks to monitor plant parameters. The nutrients come from a reservoir that incorporates a pump, as well as water level, temperature, *total dissolved solids*, and pH sensors. Finally, these sensors communicate wirelessly with a gateway, which transmits the data to a dashboard.

In the field of VF, the pH is called a *main soil parameter*, because its measurement generates *main* or primary information for soil fertilization and bioremediation processes. Moreover, the pH level is central to VF, since it influences the chemical, physical, and biological soil properties, affecting factors such as plant growth, de-nitrification, plant toxicity, bacterial activity, and soil nutrients [22,23]. In the past, several groups have reported the construction of instrumentation to enable pH measurements. For example, Jin et al. [24] developed a pH potentiometer applicable to teaching in a chemistry laboratory setting. Moreover, a pH sensor to assess the changes in cementitious materials, through a sol-gel process with an alizarin yellow as meter, has been developed [25]. Additionally, portable chemical sensors, requiring specialized processes for manufacturing, have been reported for non-invasive real-time monitoring of parameters for medical care and disease diagnosis [26,27]. Manjakkal et al. [28] integrated an electrochemical pH sensor, applicable to several industries, with a screen printed on flexible substrates through CuO nanostructures exhibiting nanorods morphology. The measurement range was established to be 5–8.5 pH units. Dang et al. [29] developed a wireless system for monitoring pH of sweat, integrated by a pair of serpentine-shaped stretchable interconnects. The authors constructed a reference electrode using graphite-polyurethane composites for biological applications. Cordoba et al. [30] reported the development of an optical sensor, which requires a high-cost external instrument to determine the pH level. Rasheed et al. [31] designed a multilayer (ZnO/Ag/ZnO) film pH sensor, which was tested as an extended gate field effect transistor. The pH detection range was demonstrated to be 2–12 pH units. Lastly, solutions using ISFET (Sensitive Field Effect Transistors) sensors, which have the advantage of being small, have been proposed. Nonetheless, with ISFET sensors, samples under study must be small, and the measuring range is limited to 10 pH units (1.5 to 11.5 pH) [32].

An essential aspect of any instrument intended for VF use is that such instrumentation must meet availability, portability, and cost-effectiveness constraints to enable global adoption. Furthermore, the global food supply chain, which by 2050 will have to increase its capacity by 60–70% due to the growth of the world population [33], would benefit greatly if connected (characteristic of *Industry 4.0* solutions) pH sensors were available. Thus, the goal of this article is to describe the implementation of a portable, cost-effective, and connected instrument that enables accurate pH measurements for VF and, more generally, *Industry 4.0* applications.

This work is divided into six sections. Section 2 deals with the theoretical background, as required to address pH sensing for global *Vertical Farming* applications. In Section 3, the instrument is described in the context of a three-layer Internet of Things architecture. Here, the circuit design for pH measurements is presented. In Section 4, the results of sensor characterization and pH measurements are presented. The discussion section, presented in Section 5, describes two modifications that can be implemented to the circuitry, in order to increase the precision of the instrument. Finally, the results of this work and future research directions are summarized in Section 6.

2. Theoretical Background

pH Sensing Aspects: Considerations for Global Industry 4.0 Applications

The term *Potentia Hydrogenii*, commonly known as pH, was originally proposed by Sørensen to describe the solution pressure of hydrogen-ions in aqueous solutions. Nowadays, the pH is conceived as a metric to quantify the activity of hydrogen-ions, a_{H^+} , in any solution. Mathematically, the pH is defined as shown in Equation (1) [34]:

$$\text{pH} = -\log a_{H^+} \quad (1)$$

The most common materials utilized for constructing electrochemical pH sensors include: 1. Glass Electrodes, 2. Metal Oxides, 3. Polymer/Carbon, and 4. Metal/Metal Oxide-Metal Composites [35]. The suitability of any of the aforementioned sensors to address global *Industry 4.0* challenges, including *Vertical Farming*, depends on worldwide availability, accessibility, and cost-efficiency of the constituting materials. Unquestionably, the *Glass Electrode* is a front-runner by fulfilling the requirements needed for global adoption of pH sensing. Glass electrodes [36], including the well-known *silver | silver-chloride* (Ag | AgCl) arrangement, implement a two electrode setup. These potentiometric systems consist of working and reference electrodes. Furthermore, the main working concept of these pH sensors relies on measuring equilibrium conditions at the surface of the working electrode. Under equilibrium conditions, *Nernst's Law*, shown in Equation (2) applies, and describes the (half) cell potential in terms of the activity of the electroactive species [37]:

$$E_{eq} = E^0 + \left(\frac{RT}{nF}\right) \ln\left(\frac{a_0}{a_R}\right) = E^0 + 2.303\left(\frac{RT}{nF}\right) \log\left(\frac{a_0}{a_R}\right) \quad (2)$$

where

E_{eq} represents the electric potential at equilibrium [V],

E^0 denotes standard potential [V],

R is the universal gas constant; $8.314 \text{ [J mol}^{-1} \text{ K}^{-1}]$,

T represents the temperature [K],

n denotes the electrons number,

F is the Faraday constant; $96,485 \text{ [C mol}^{-1}]$,

a_0 represents the activity of the oxidizing agent,

a_R denotes the activity of the reducing agent.

In a practical setting, on one side of the sensor, the reference electrode is exposed to a well-known and constant solution of hydrogen-ion activity, e.g., a buffer solution. On the other side of the sensor, the electrode is in contact with the pH solution under study. Due to the aforementioned sensor design, the contribution of one (i.e., the reference) of the electrodes is known, and Equation (2) can be rewritten as a function of the pH under study, as expressed in Equation (3):

$$E = E^0 - \left(\frac{2.303 \times RT}{nF}\right) \text{pH} \quad (3)$$

Detection electronics, signal conditioning and acquisition, as well as wireless communications of the electrical signal are critical aspects in sensing (pH) variables for global VF (and *Industry 4.0*) applications, especially due to the fact that a majority of the (farming) operations occur in places with scarce access to technology. Therefore, the instrumentation required to accurately measure pH for global *Industry 4.0* applications is far from trivial, requiring accurate characterization of the expected signals and a suitable design that is applicable to the setting where the technology will be implemented.

Taking these considerations for global VF applications into account, an accurate characterization of the expected signal is indispensable. For a standard and globally available *silver | silver-chloride* reference electrode configuration, the electrochemical redox response is well known (Ag | AgCl standard potential being 220 mV [38]) and involves the

generation of only one electron. Consequently, the relationship between electric potential and pH is linear, and the slope is a function of temperature (refer to Equation (3)). Assuming a working temperature of 25 °C, the ideal Nernst response is shown in Equation (4):

$$E = E^0 - 59.16 \times \text{pH} [\text{mV}] \quad (4)$$

As presented in this section, novel materials have been proposed and developed to measure the pH for various applications. Some of these materials exhibit a sensitivity (i.e., the slope in the last expression) metric that is greater than the value of the Nernstian response, described in Equation (4). Nevertheless, despite material and manufacturing complexities, most sensitivity values oscillate around 40 to 80 [mV/pH]. Furthermore, in global *Industry 4.0* applications, including VF for developing countries, access to electrodes made with novel materials is scarce, limiting sensitivity to values below the Nernstian response, 59.16 [mV/pH]. Therefore, the design and implementation of portable and cost-efficient solutions to accurately measure pH in global *Industry 4.0* applications represent a challenge.

In this work, we present a potentiometric pH measurement instrument that is compatible with readily available glass electrodes (as well as other less conventional sensors), and that implements an optimal electronic design by being accurate, portable, cost-efficient, and *Industry 4.0* ready for global applications.

3. Materials and Methods

Internet of Things (IoT) is a key enabling technology for *Industry 4.0* applications. No unified or standardized agreement has been reached with respect to IoT architectures. Nonetheless, every IoT architecture should implement at least three layers [39]. More complex architectures, including four- or five-layered ones, have also been proposed [40]. The instrument described in this work is unique, compared to other pH sensing devices, because it incorporates a three-layer IoT architecture with *Perception*, *Network*, and *Application Layers*.

3.1. Materials

In Figure 1, we depict the block diagram of the cost-effective and portable instrument to enable accurate pH measurements for global VF and, more generally, *Industry 4.0* applications, as proposed and implemented by our group. The instrument described in this work is unique, compared to other pH sensing devices, because it incorporates a three-layer IoT architecture with *Perception*, *Network*, and *Application Layers*.

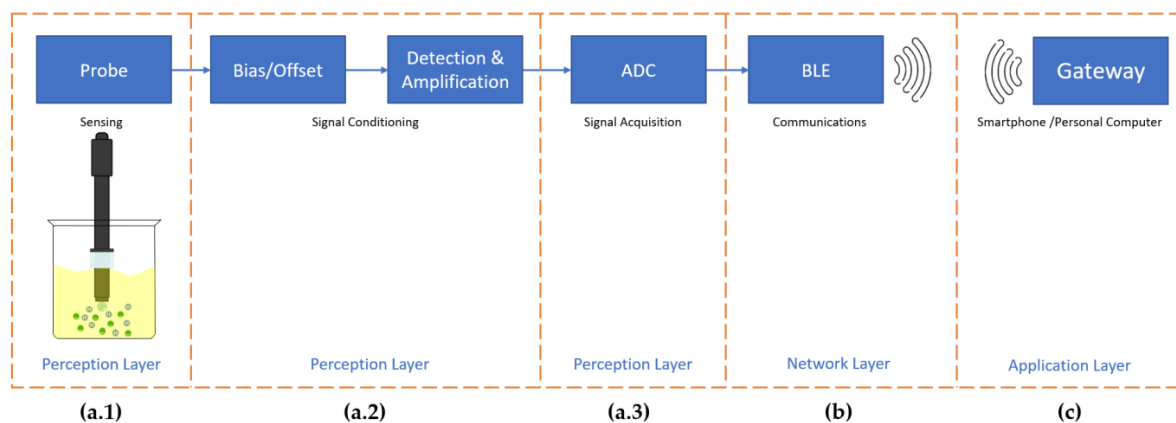


Figure 1. The cost-effective and portable pH instrument has been implemented in a three-layer IoT architecture, consisting of (a) *Perception*, (b) *Network*, and (c) *Application Layers*. The *Perception Layer* is further divided into: (a.1) *Sensing*, (a.2) *Signal Conditioning*, and (a.3) *Signal Acquisition* stages. The *Network Layer* has been enabled by means of a Bluetooth (BLE) *Communications* stage. The *Application Layer* utilizes a gateway, in the form of a *Smartphone* or a *Personal Computer*, for user interaction.

As illustrated in Figure 1, the three-layer architecture of the instrument incorporates: (a) *Perception Layer*, (b) *Network Layer*, and (c) *Application Layer*. The *Perception* or *Physical Sensor Layer* is further divided into: (a.1) *Sensing*, (a.2) *Signal Conditioning*, and (a.3) *Signal Acquisition* stages. Meanwhile, the *Network Layer*, used to connect the pH sensor to other sensors, network devices, or servers, is implemented through a *Wireless Bluetooth (BLE) Communications* stage. Finally, the *Instrument Application Layer*, which is in charge of providing useful information to the user, is enabled by means of a smartphone or a personal computer. Hereafter, we describe the materials necessary to implement the sections of the accurate, cost-effective, and portable instrumentation for pH measurements.

3.1.1. Perception Layer—Sensing Stage

We employ a *silver | silver-chloride, Ag | AgCl*, glass electrode in a potentiometric arrangement, which is readily available and cost-effective. The implemented sensor (Hinotek, Ningbo, China, E201-BNC) consists of a working electrode in the form of a glass ball, filled with a well-known buffer solution, which is in contact with the sample under study. The reference electrode also interacts with the solution of unknown pH. The sensor is protected by a cover and maintained in a storage solution, which is central to ensure sensor performance over time. A schematic of the pH sensor is depicted in Figure 2.

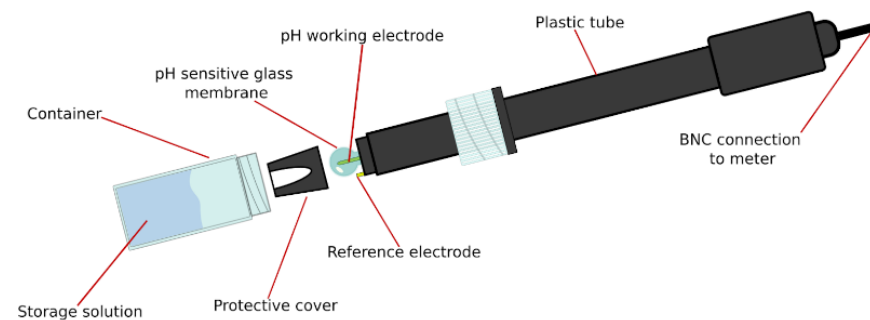


Figure 2. The implemented sensor consists of: a. Working electrode in contact with sample under study; b. Reference electrode interacting with solution of unknown pH; c. Protective cover; d. Storage solution; and e. Standard BNC connector for interoperability.

Any other pH detector (including those implementing novel materials) in a potentiometric arrangement would, despite accessibility and/or availability constraints, be compatible with the instrument described in this work, provided it has a standard BNC connector. Such a connector was selected to ensure interoperability and to facilitate signal conditioning interfacing.

3.1.2. Perception Layer—Signal Conditioning and Signal Acquisition Stages

As clearly seen from Equation (4), alkaline solutions tend to generate negative potential differences. Meanwhile, acidic solutions will have a positive trend, in terms of the voltage generated by the sensor. Therefore, in order to ensure that the electrical waveform is adequate for analog to digital conversion (ADC), an offset voltage must be implemented in the signal conditioning stage. As illustrated in Figure 3, a divider network with a stable voltage input (Texas Instruments, Dallas, TX, USA, TL431) of 2.5 V defines the bias voltage. This offset voltage can be varied by means of a potentiometer (RV1). In the discussion section, we present key modifications to the passive components of this bias stage of the signal conditioning circuitry, which serve to optimize pH detection.

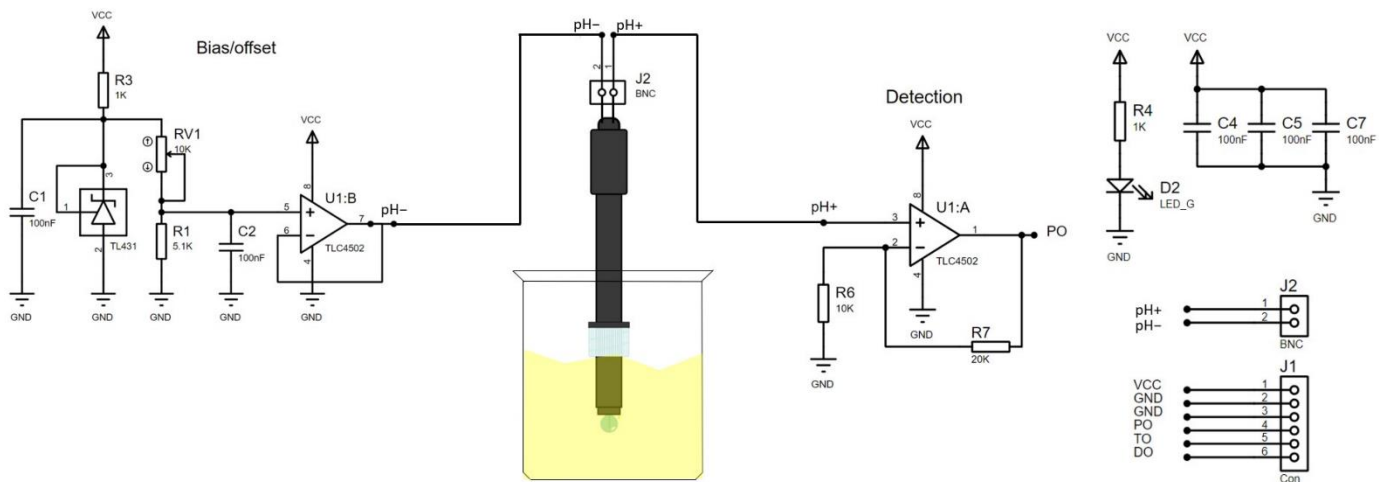


Figure 3. The signal conditioning stage is constructed by implementing an offset section, followed by a detection/amplification stage. The sensor is coupled using an array of precision op-amps in buffer and non-inverting amplifier configurations to ensure adequate performance.

Considering that a potentiometric system is in place, pH measurements should be ideally performed in equilibrium, as emphasized in Equation (2). Therefore, the electrical current generated between working and reference electrodes should be as negligible as possible. This implies that the impedance of offset and detection stages should be various orders of magnitude greater compared to the pH sensor impedance.

The instrument employs an array of precision operational amplifiers, op-amps (Texas Instruments, TLC4502), with an input impedance of $1 \times 10^{12} [\Omega]$ and a typical bias current of 1 [pA]. Such a configuration ensures that negligible current flows through the sensor as required by the potentiometric design. Finally, the amplification section is configured as a conventional non-inverting amplifier with the gain determined by resistors R6 and R7, as depicted in Figure 3. In order to facilitate global VF applications, the complete signal conditioning stage can be implemented in a single electronic module (DIY More, Hong Kong, China PH-4502C). A thorough revision of such integrated modules is suggested, in order to determine expected offset, detection, and amplification performance. Finally, breadboard implementations can be constructed by following the schematic of Figure 3.

The electrical signal generated by the instrument proposed in this work is the sum of the bias voltage plus the potential difference generated by the pH sensor, as seen in Figure 3. This signal is amplified and acquired by the ADC of a microcontroller. In our case, an ATmega328P (Atmel Corporation, San Jose, CA, USA) microcontroller built into an Arduino UNO board (Smart projects, Ivrea, Italy, Arduino UNO) was used. It is important to note that, in order to enable global adoption, practically any standard microcontroller, such as those of the STM32 Family (STMicroelectronics, Grenoble, Auvergne-Rhône-Alpes, France), the nRF52 series (Nordic VLSI, Trondheim, Trondheim Fjord, Norway), or other member of the ATmega series (Atmel Corporation, San Jose, CA, USA), can be equally employed. Similarly, other integrated modules can be utilized to replicate this instrumentation locally.

3.1.3. Network Layer—Bluetooth Wireless Communications Stage

The *Network Layer* enables the pH sensor to connect to other devices such as gateways (e.g., in the form of smartphones or personal computers) or even other sensors. Such connectivity is characteristic of *Industry 4.0* applications. In the instrument described in this work, a Bluetooth radio version 2.0 (Linvor, Jinan city, Shandong, China, LV-BC-2.0) enables wireless transmission of pH data, and serves as the *Network Layer*. The radio, implemented in a breadboard (Olimex, Plovdiv, Bulgaria, BLE HC-06) for ease of integration, is a Class 2 device, and exhibits a maximum communication range of 10 m [39]. This range is sufficient for isolated VF applications. However, for distributed VF applications or, more generally, other *Industry 4.0* applications, a Class 1 Bluetooth device can be employed to yield a

range of 100 m. In fact, for conventional farming, the Bluetooth technology enables a very desirable feature: *Mesh Networks* [40]. In such a topology, a rather large area (e.g., 1000 m²) can be covered with a handful of Bluetooth radios. Any gateway, functioning as part of the *Application Layer*, which supports Bluetooth communications, as specified in this section, can interface with the instrumentation, potentially minimizing deployment challenges encountered in global *Industry 4.0* applications.

3.1.4. Integration of the Portable pH Instrument

Figure 4 displays the layout and a representative picture of our portable pH instrument, as well as the integration required to enable accurate pH measurements for global VF applications. To integrate the overall solution six main components are needed: 1. Glass electrode for pH sensing with standard BNC connector; 2. Signal conditioning module; 3. Bluetooth communications module; 4. Integration breadboard; 5. Signal acquisition and processing module; and 6. Power supply.

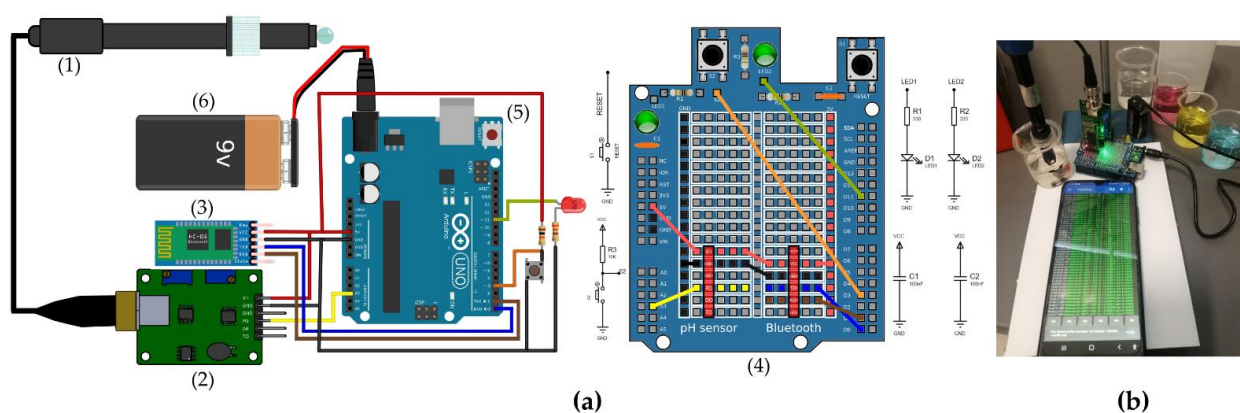


Figure 4. (a) The pH instrumentation for global VF applications consists of six main components: (1) Glass electrode; (2) Signal conditioning module; (3) Bluetooth communications module; (4) Integration breadboard; (5) Signal acquisition and processing module; and (6) Power supply. (b) Representative photo.

Figure 4a provides a detailed integration (i.e., wiring) diagram to ensure adequate signal processing, as well as the intermediate breadboard needed to assemble the components that constitute the instrument. Finally, Figure 4b presents a representative picture of the portable instrument for pH measurements.

3.2. Methods

3.2.1. pH Sensor Characterization

The pH of a solution under study can be determined after a meticulous calibration. In order to characterize the pH sensor, the potential difference over the two electrodes must be measured, and related to the hydrogen-ion activity of reference solutions.

Three pH buffer solutions (Mallinckrodt Baker, Hampton, NJ, USA, manufacture date 31 August 2020) with a 2-year validity certification (at 25 °C) and traceable to NIST standards were used. The standard buffer solutions employed in the calibration of our instrument were: 1. Biphthalate; 2. Phosphate; and 3. Borate. Correspondingly, the pH and certified range values for the buffer solutions were 4 [3.96, 4.04]; 7 [6.96, 7.04]; and 10 [9.99, 10.01]. Utilizing the batch information of our buffer solutions, the pH reference values for our calibration procedure were: 3.99, 6.98, and 10.00.

The characterization method is divided into two phases. In phase one, the sensitivity of the pH sensor is determined with a conventional voltage meter, such as a multimeter. It is important to note that the instrument input impedance should be high, and the noise performance optimally below the mV range for accurate calibration. In phase two, the signal conditioning stage, as described in this work is employed, in order to quantify

the modified (i.e., including bias and amplification effects) sensitivity of the pH sensor. Hereafter, the methods for both phases are described.

Phase I does not include the signal conditioning stage. First, the pH sensor is attached to the measuring device using the BNC connector. For this phase, a multimeter (Steren, Ciudad de México, Mexico, MUL-605) is employed to determine the voltage, irrespective of polarity, as a function of buffer solution. Next, the calibration curve that describes the linear behavior of the sensor is calculated by using regression techniques. As seen from Equation (4), the derived slope will serve to relate pH as a function of (sensor) voltage.

In Phase II, the signal conditioning stage is included. Nonetheless, the above methodology remains practically the same. One of the differences is that in the first step, the pH sensor is attached to the signal conditioning module using the BNC connector. Then, the circuitry of Figure 3 is employed to measure the voltage as a function of buffer solution. Next, the calibration curve that describes the linear behavior of the sensor is obtained by employing regression techniques. Here another difference is in place. The pH is still related to a modified potential difference, which includes the effects of the signal conditioning stage: bias and amplification. The modified potential difference is obtained by dividing the output voltage by the gain and subtracting the bias voltage. The derived slope will serve to relate pH as a function of (instrument) voltage. Finally, it is important to note that, irrespective of the calibration method, the overall cleanliness and mechanical stability, while measuring, of the working electrode are key factors to obtain accurate calibration results.

3.2.2. Preparation of Signal Conditioning, Acquisition, and Transmission

The procedure implemented to utilize the signal conditioning, acquisition, and transmission stages is as follows. First, the wiring of the instrument is performed, as shown in Figure 4a. It is relevant to note that this step defines the performance of the signal acquisition stage, if an external voltage is used. In our case, this parameter was set to 5 V using the microcontroller code. Then, the offset voltage of the instrument is tuned by cautiously adjusting the potentiometer, RV1 in Figure 3, thus accounting for the ADC configuration previously mentioned. Finally, BLE transmission of sensed data is facilitated by means of the microcontroller code, which implements two modalities: *Calibration* and *Measurement*. In *calibration* mode, the user is enabled to characterize the sensor (refer to Section 3.2.1) by employing the three buffer solutions. The resulting parameters are stored in the instrument memory for future use. In *measurement* mode, the instrument acquires arbitrary voltage values, and converts such information to pH values. pH information is then sent serially to the Bluetooth radio, which transmits wirelessly the data to a gateway (i.e., personal computer or smartphone) for further processing.

3.2.3. Methodology to Assess the pH of Arbitrary Solutions

The first step to measure the pH of a selected sample is to perform the calibration of the probe, refer to Section 3.2.1. Here, sensor cleanliness is crucial. Second, the sensor is connected to the instrument, and the signal conditioning, acquisition, and transmission stages are prepared as mentioned in Section 3.2.2. Once this has been performed, the instrument is ready for measurements. Nevertheless, the sample must be prepared and the chemical integrity of the same must be ensured. In order to perform pH evaluation, mechanical stability must be guaranteed. In the discussion section, we elaborate further on the implications of unstable systems, which are likely to occur in global VF settings.

A *simple-to-use* interface was implemented, by means of a push-button (S2), to select the operation modality. A light emitting diode (LED2) is used to indicate operation mode, and for general user interaction. Once instrument and sample are ready, the user selects an operation mode, by means of S2, and performs the pH measurement. Such measurement is then transmitted to the gateway of interest. The microcontroller code and exemplary pH measurements are available upon request to the authors.

The microcontroller code and exemplary pH measurements are available upon request to the authors. Furthermore, calibration code may be found in the Supplementary Materials section of this work.

4. Results

4.1. Signal Conditioning Characterization

Potential differences with negative and positive polarities will ensue for alkaline and acidic solutions, respectively. Furthermore, in order to optimize performance, the full dynamic range of the ADC should be used. This condition implies that the minimum bias voltage should ideally match the potential difference for the most alkaline solution possible. Additionally, optimally, the maximum offset value would match the potential difference for the most acidic sample.

The minimum offset voltage is obtained by selecting the greatest resistance value of the potentiometer, RV1, in Figure 3. Recalling that a 2.5 V stable source feeds the voltage divider network, by simple inspection, the minimum bias voltage is determined to be 840 mV. The maximum offset, however, depends not only on the divider network (with a theoretical value of 2.5 V), but also on the amplifier and acquisition setup. From Figure 3, it is trivial to anticipate a three-fold gain for the amplification stage. Furthermore, assuming a conventional ADC configuration with an analog reference voltage V_{AREF} of 5 V, the maximum input signal will be given by $V_{AREF}/GAIN$, or quantitatively 1.67 V.

A device exhibiting Nernstian response would have a full detection range of ± 414 mV, centered ideally at 0 V for a neutral pH. In global VF applications, the aforementioned range denotes theoretical extrema of practically all available sensors.

Combining the effects of bias and electrode response, the signal conditioning characterization is obtained before and after the amplification stage. The minimum theoretical voltage should be 426 mV before amplification and 1.278 V after. Meanwhile, as stated above, the maxima have an additional restriction imposed by the ADC. Thus, the maximum voltage should be 1.67 V before amplification and 5 V after. This analysis serves to demarcate the working bias range of the signal conditioning stage. Assuming the Nernstian response, end users can select any offset voltage in the 840–1250 mV range. From this analysis, we detect an area of improvement; namely, the optimization of the ADC dynamic range. Such improvement is addressed in the discussion section.

4.2. Sensor Characterization

As described in Section 3.2.1, and shown quantitatively in Figure 5, the pH sensor is characterized in two phases: Figure 5a, using a multimeter and Figure 5b, employing the instrumentation described in this work. During the first ten seconds, refer to Figure 5, the sensor remains outside of the sample, and then the electrode is exposed (i.e., introduced) to the solution under test. It is important to note that this was performed for both configurations. Then, we let the sensor stabilize and perform the measurements for a period of 60 s, while acquiring data every 0.25 s. Table 1 presents, for both sensor characterization phases, the statistical measures obtained for voltage and pH after the aforementioned 60 s period.

Table 1. Statistical parameters derived from pH sensor characterizations: Phase I and Phase II.

pH *	Phase I. Multimeter **	Phase II. Instrumentation **	
	E{V} [mV] ***	E{V} [V]	$\sigma\{V\}$ [V]
4	164.74302	3.04761449	0.000487422
7	4.48031	2.5272936	0.000456076
10	−166.07790	2.01269855	0.000459554

* The certified (Batch/Product Numbers: B38W00/5657, B35W06/5656, and B35W00/5655) pH values of the buffer solutions utilized in this work were 3.99, 6.98, and 10.00. The systematic uncertainty of the pH of buffer solutions establishes a limit in the precision (in the 0.01 range) of pH measurements that can be achieved with this method. ** Here, E{V} and $\sigma\{V\}$ stand for expected value and standard deviation of random variable V, which represents the measured voltage or electrical potential in mV or V. *** The measurement range for the voltage meter was set to automatic, and did not surpass ± 400 mV. From the manufacturer datasheet, the precision of the readings is expected to be 0.5% within this range.

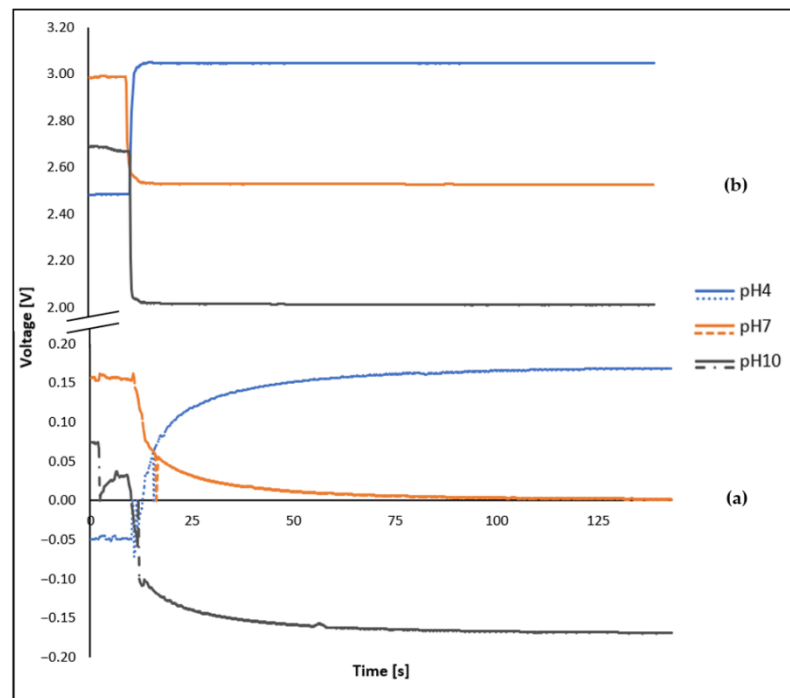


Figure 5. The sensor characterization is performed in two different phases: (a) utilizing a multimeter and (b) employing the instrumentation described in this proposal.

As noted in Section 4.1, from Table 1 and Figure 5, we confirm that, for our sensor, the response to neutral pH solutions is practically centered at 0 V. Additionally, for the configuration of the instrument, the bias voltage was measured to be 840 mV. Thus, the expected quantitative voltage for a neutral solution, at the instrument output, is straightforwardly determined to be 2.52 V, which matches precisely the measured value.

Considering that the instrument will bestow information comparable to that shown in Table 1, the calibration curve is obtained by performing a linear regression to this data. In Equation (5), the linear regression is presented. Furthermore, in Figure 6, we depict the calibration curve for our pH sensor.

$$\text{pH} = -5.791 V_{out} + 21.647 \tag{5}$$

where V_{out} represents the output instrument voltage in [V].

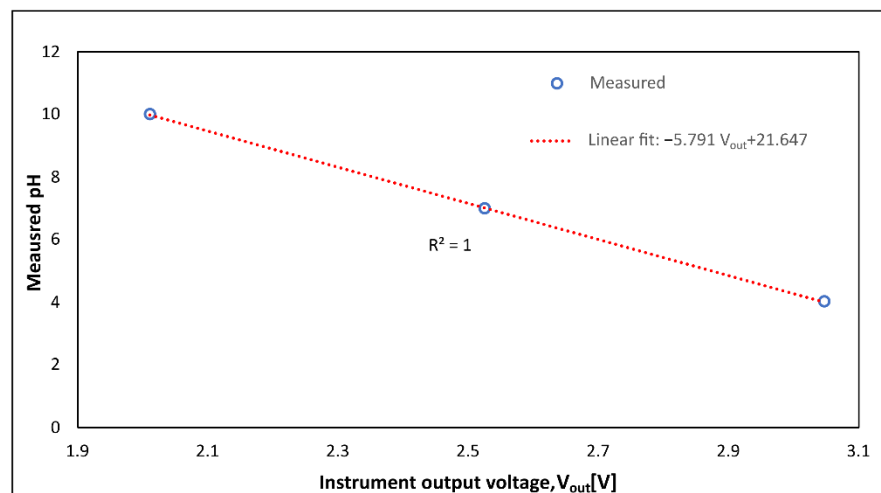


Figure 6. The calibration curve enables the direct measurement of pH from the instrument output.

In Section 3.1.2, the importance of the instrument impedance to obtain accurate measurements was emphasized. Additionally, in the design proposed in this work, we placed special emphasis on this respect. In fact, the multimeter datasheet (Steren, Ciudad de México, Mexico, MUL-605) reports an input impedance of 10 M Ω , which is significantly lower than the impedance in our proposal. By carefully following the procedure for Phase II, described in the preceding section, the instrument (without offset and amplification effects) sensitivity can be calculated. This information is shown in Table 2.

Table 2. Statistical sensitivity parameters derived from pH sensor characterization: Phase II.

Phase II. Instrumentation *	
pH	E{V} [mV]
4	173.666667
7	0
10	-171.666667

* Here, E{V} is the expected value of a random variable V, which represents the measured voltage in mV.

A device exhibiting Nernstian response would have a detection range of ± 177 mV, ideally centered at 0 V, for a pH range of ± 3 units. Comparing the theoretical Nernstian response to the values presented in Table 2, a maximum deviation of 6 mV for the proposed instrument is observed. Moreover, translating the information presented in Table 2 to the sensitivity metric (i.e., voltage per single pH unit [mV/pH]), it is simple to demonstrate a measured (average) sensitivity of 57.56 [mV/pH]. Comparing this value to the Nernstian response, see Equation (3), the instrument sensitivity is 1.6 units below the reference parameter. By simple mathematical calculation this represents a 97.3% percent “compliance” with respect to the optimal Nernstian response. It is, thus, concluded that the proposed pH sensor characterization described in this work may enable the creation of a precise and portable instrument for global VF applications requiring pH measurements.

4.3. Accurate pH Measurements for Global Industry 4.0 and Vertical Farming Applications

In order to validate the accuracy of our portable instrumentation, as intended for global VF (and *Industry 4.0*) applications, a laboratory grade pH device (Ohaus Corporation, Parsippany, NJ, USA, AB33M1) was selected as gold standard. Thirteen samples with varying pH values were utilized. For every measurement, a rigorous process involving cleanliness, temperature stability, calibration, and mechanical stability of the probe was implemented. Figure 7 depicts the results of the instrument presented in this work to enable accurate pH measurements for global *Industry 4.0* and VF applications. In order to ensure global VF applicability, the cost of the device is important. In our case, the cost (uelectronics) of the instrument was ~60 USD. In contrast, the gold standard costs ~715 USD (Viresa); i.e., $\sim 11.5\times$ more expensive. Thus, our solution is cost-effective, portable, and accurate.

Using the information depicted in Figure 7, the average and median absolute deviations (reference minus measured pH) are 0.057 and 0.063 pH units, respectively. Meanwhile, the standard deviation of the absolute deviation is 0.03 pH units. For the acidic substance exhibiting the lowest pH value, the maximum relative error is 5%. In contrast, alkaline substances have relative errors that are as low as 0.3%. Figure 7 depicts error bars that describe the absolute deviations of measured and reference data. As noted before, various error bars are not easily distinguishable due to instrumentation performance. In any case, the accuracy and applicability of the proposed instrument is clearly established.

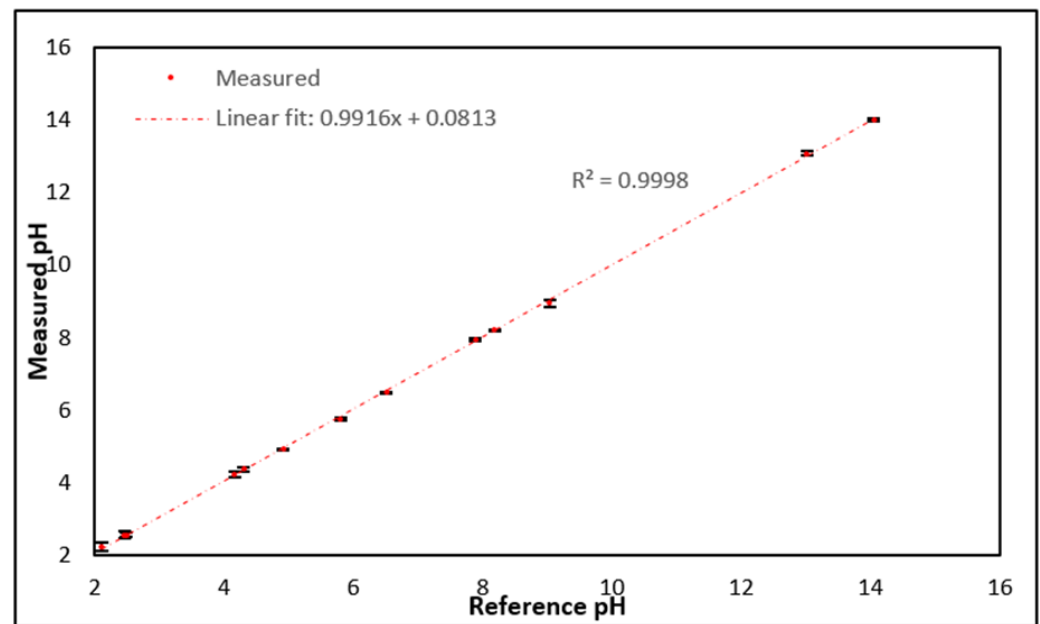


Figure 7. The performance of the portable instrumentation for pH measurements is established by comparing our results to those of a reference instrument (Ohaus, AB33M1). The solutions utilized for this experiment, in ascending order of pH value, commencing from the most acidic one, are given as follows: a. Lemon juice, b. Cola soda, c. Vinegar, d. Orange juice, e. Beer, f. Coffee, g. Tea, h. Milk, i. Tap water, j. Human saliva, k. Hand soap, l. Sodium hypochlorite, and m. Sodium hydroxide.

5. Discussion

Various research groups have proposed different systems for pH sensing. Table 3 presents a comparison of sensor features, including *pH sensitivity* and *range*, *application area*, *cost*, and *portability*, as required for global applications. This analysis serves to present the results of this work in the light of previous advances reported in the scientific literature. The features of the laboratory grade apparatus, which was employed as gold standard, are also included for completeness.

Table 3. Comparison of pH sensor features as required for global applications.

pH Sensing Materials	pH Range	pH Sensitivity	Application Area	Cost (USD)	Portable	Global Access	Ref.
CuO Nanorods	5–8.5	0.64 $\mu\text{F}/\text{pH}$ at 50 Hz	Biological, Food, Medicine, Agriculture	N/A	No	No	[28]
Graphite-polyurethane composite (Ag AgCl) EGFET (ZnO Ag ZnO)	5–9	$-11.13 \pm 5.8 \text{ mV}/\text{pH}$	Health Monitoring *	N/A	N/A	N/A	[29]
Glass electrode (Pd PdO)	2–12	$0.62 \mu\text{A}^{1/2}/\text{pH}$	Health Monitoring	N/A	N/A	N/A	[31]
Carbon fiber thread electrodes coated with self-healing polymers (Ag AgCl and Pt wire)	N/A	51 mV/pH	Laboratory Instruction	\$50 **	Yes	No **	[24]
Sol-gel-entrapped TiN-gate ISFET	3.89–10.09	58.28 mV/pH	Health Monitoring and Disease Diagnostics	N/A	Yes	No	[27]
Ohaus AB33M1 (Ag AgCl)	10.2–12	N/A	Cementitious materials	N/A	N/A	N/A	[25]
Glass electrode (Ag AgCl)	4–10	53.98 mV/pH	Medicine and Biological Industries	N/A	N/A	N/A	[41]
Glass electrode (Ag AgCl)	1–14	N/A	Not restricted	\$715	No	No	[TW] ***
Glass electrode (Ag AgCl)	2–14	57.56 mV/pH	Not restricted	\$60	Yes	Yes	[TW] ***

* The device was originally reported for *sweat monitoring* applications. ** Reported cost refers to hardware electronics, the design of which is intended for a laboratory setting and would require modularity to enable global adoption. *** TW = This Work.

As seen from the data in Table 3, most of the end applications are related to biological areas. Additionally, a crucial aspect is that measurement range are limited, and that sensors have been designed, developed, and implemented for specific tasks. In contrast, it is clear from Table 3 that the instrumentation described in this work provides the features of *accuracy, measurement range, portability, cost-efficiency, and adaptability*, necessary to address global *Vertical Farming* and *Industry 4.0* pH sensing challenges. Nonetheless, some systems, such as those reported by Rasheed et al. [31] and Jin et al. [24], exhibit similar characteristics in terms of measuring range or cost (i.e., specific features needed for global adoption). Having a single instrument that can offer the complete set of features needed for global adoption is a key contribution of this work.

The instrumentation described in this work enables precise determination of the pH, with an expected absolute deviation of 0.06 pH units and a standard deviation of 0.03 pH units. The precision required of pH measurements is intrinsically related to the task under consideration. For instance, in the field of hydroponic farming (hydroponics is an advanced technique for plant and vegetable production that utilizes water instead of soil as growing matrix [42], implementable in a *Vertical Farming* setting), the pH level must be maintained in the 5.5 to 6.8 range [42]. Furthermore, the detection of minor changes in the pH level significantly impacts water quality, and thus, the main nutrients of these systems. The instrument presented in this work enables accurate detection of pH variations of 0.1 pH units, with a 68% confidence interval, for hydroponic farming. Hereafter, a brief discussion of the sources of uncertainty, within our instrument, is presented for those applications requiring more stringent pH control.

First, with respect to the actual sensor, the efficiency of the electrode can degrade due to the manufacturing process (better vs worse quality), glass membrane, reference cables (e.g., electrical interference or RF coupling), and especially maintenance. A decrease in performance has been validated, by our group, if the electrode is poorly maintained (i.e., cleaned). To counteract this problem, the calibration, as described in this work, was implemented. More concretely, in order to ensure accurate readings, the calculation of the *sensor “compliance”* metric, is advisable. For the case reported in this work, such a metric was demonstrated to be 97.3%.

Next, the impact of *Signal Conditioning* and *Acquisition* stages, which are closely interrelated, is addressed. In the current version of the pH instrument, refer to Section 4.1; the offset voltage is fixed to its minimum value of 840 mV. This places a restriction on the usable detection range of the ADC to 48%; namely, from 1.32 to 3.73 V (corresponding to pH values from 14 to 0 units). Figure 8 depicts a two-step approach to significantly improve the signal conditioning circuitry. First, the feedback resistor, R7, can be substituted (e.g., 10 k Ω) to set the amplification factor to a different value (e.g., GAIN = 2), and the analog reference voltage can be set to 2.56 V. By implementing this first step, the usable detection range of the ADC becomes 65%; that is 0.83–2.51 V. Second, the minimum offset voltage of the divider network can be reduced to a different value (e.g., 420 mV). This is achieved by replacing the fixed resistor, R1, with a 2 k Ω component. By selecting the amplification factor correctly, the usable detection range can be optimized to 98% (i.e., in the 0–2.52 V range), which is approximately a two-fold improvement.

As noted throughout this work, the expected magnitude of the detected signal will approximate the Nernstian response, with a maximum of 59.16 mV per pH. For our instrument, the measured sensitivity was demonstrated to be 57.56 [mV/pH]. Thus, a difference of 10 mV in the sensor signal implies a variation of ~ 0.175 pH units. Various sources can induce voltage variations of this magnitude, including the communications and ADC stages.

The *Network Layer*, or wireless communications stage, is not only necessary to enable transport of pH information, but rather indispensable to minimize coupling and/or layout effects in the instrumentation. In fact, pH information could also be sent to a personal computer (or smartphone) by means of wired (e.g., serial) communications. However, voltage variations on the 10 mV range due to coupling errors are commonly encountered

in wired communications. As noted before, such variations would induce an error that is almost twice the value of the instrument accuracy.

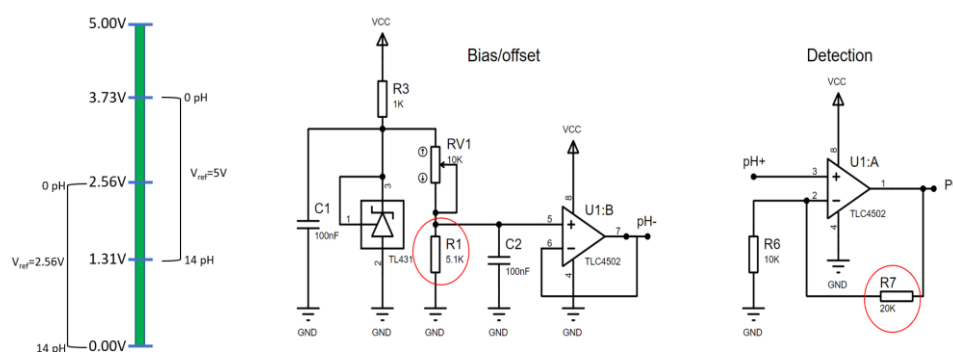


Figure 8. The signal conditioning stage can be improved by optimizing the usable detection range of the ADC. We propose to modify the feedback resistor and the (fixed) voltage divider network resistor to improve the performance by a two-fold factor: from 48 to 98% usable detection range.

Moreover, the evaluation of the dynamic range of the ADC is important because this establishes a minimum detectable voltage (i.e., pH). Thus, the measurement of potentials below a certain threshold is not plausible, and the system is said to be ADC-limited. Furthermore, various deviations inhibit ideal performance of ADCs. The absolute accuracy of an ADC serves to quantify: gain error, offset deviations, differential error, non-linearity, and quantization error. The ideal value of the absolute accuracy is ± 0.5 LSB.

In our instrument, a 10-bit ADC (Atmel Corporation, San José, CA, USA, ATmega328P) is utilized with a reference conversion voltage of 5 V and a typical absolute accuracy of ± 2.2 LSB. This implies a minimum detectable voltage of 4.88 mV, with ideal and typical absolute accuracies of ± 2.44 mV and ± 10.74 mV, respectively. As is the case with other deviation metrics, statistical methods can be utilized to reduce these errors.

The mean sensitivity of our instrument can be obtained from the absolute values of Table 2, and is equal to 172.67 [mV/pH]. This maps directly to the usable conversion range of the ADC, which is 2.41 V, over the full range of pH values. Therefore, we expect the minimum detectable pH value to be 0.028 units, with ideal and typical absolute accuracies of ± 0.014 pH units and ± 0.062 pH units, respectively. From this analysis and the results presented in this work, we can conclude that the current instrument design is ADC-limited. A straightforward improvement in the instrument can be implemented by using ADCs with greater dynamic ranges. For instance, the STM32L041 (STMicroelectronics, Grenoble, Auvergne-Rhône-Alpes, France) incorporates a 12-bit ADC, which would reduce by a four-fold factor the minimum detectable voltage, improving absolute accuracy proportionally. In such a setup, the minimum detectable pH increment would be 0.007 units, with ideal and typical absolute accuracies of ± 0.0035 pH units and ± 0.015 pH units, respectively.

Global (conventional and *Vertical Farming*) solutions are necessary worldwide. Such systems need to be robust in order to ensure adoption. Even in a controlled laboratory setting mechanical instabilities are readily recognized, refer to Figure 5. Due to the fact that minimal increments in sensor readings convert into significant pH variations, such instabilities impact significantly the recovered values. Our group has recently proposed an artificial intelligence (AI) approach to compensate for these types of scenarios [43,44].

6. Conclusions and Future Work

In this work, the implementation of a cost-effective and portable instrument, which enables accurate pH measurements for global *Vertical Farming* applications, has been described. By performing a well-designed calibration of the sensor, near Nernstian response, in this case 57.56 [mV/pH], was demonstrated. The instrumentation was compared to a laboratory gold standard, which is at least ten times more expensive, and was shown to be accurate in determining the pH of substances in the 2–14 range. Furthermore, the

instrument yields precise pH results with an average absolute deviation of 0.06 pH units and a standard deviation of 0.03 pH units. Compared to previous research efforts, the instrumentation is unique because it incorporates a three-layer IoT architecture with *Perception*, *Network*, and *Application* Layers. Additionally, the design is optimal for worldwide adoption by consisting of four modular stages: sensing, signal conditioning, signal acquisition, and communications. The design of the instrument was shown to be ADC-limited, with a minimum detectable value of 0.028 pH units, and a typical absolute accuracy of ± 0.062 pH units. In order to overcome this limitation, a means to improve performance was presented by meticulously designing the bias and amplification circuitry of the signal conditioning stage, and by optimizing the signal acquisition section of the instrument. The next steps in our research include the implementation of an AI algorithm to detect and compensate for mechanical instabilities of the instrument, and to incorporate other critical sensors, such as total dissolved solids meters, for VF applications.

Supplementary Materials: The calibration code information can be downloaded at: https://pabellon.tecnm.mx/LIA/productos_generados.html#Trabajos_realizados (accessed on 30 June 2022).

Author Contributions: Conceptualization, R.H.-M., E.O.-G. and P.V.-J.; methodology, R.H.-M., E.O.-G. and P.V.-J.; software, R.H.-M., N.E.-G. and M.M.R.; validation, R.H.-M., E.O.-G. and P.V.-J.; formal analysis, R.H.-M., E.O.-G., N.E.-G., J.A.D.-A., M.M.R. and P.V.-J.; research, R.H.-M., N.E.-G. and P.V.-J.; resources, E.O.-G., J.A.D.-A. and P.V.-J.; data curation, R.H.-M., N.E.-G. and P.V.-J.; original drafting-drafting, R.H.-M., N.E.-G. and P.V.-J.; drafting-revising and editing, E.O.-G., M.M.R., J.A.D.-A. and P.V.-J.; visualization, R.H.-M., N.E.-G. and P.V.-J.; supervision, E.O.-G., N.E.-G., J.A.D.-A., M.M.R. and P.V.-J.; project management, R.H.-M., E.O.-G., N.E.-G. and P.V.-J.; fund raising, E.O.-G. and N.E.-G. All authors have read and agreed to the published version of the manuscript.

Funding: We acknowledge the support of the Consejo Nacional de Ciencia y Tecnología (CONACYT) in Mexico for supporting this work through funds for projects INFRA-2016-01, Project No. 270665. CB-2016-01, Project No. 287818. Additionally, we acknowledge the support to the Government of the State of Aguascalientes, and the Instituto para el Desarrollo de la Sociedad del Conocimiento del Estado de Aguascalientes (IDSCEA) through the Technological Innovation Fund for projects FEIT-AGS-2020-20-17, FEIT-AGS-2020-20-18 and 029-FEIT-2021.

Institutional Review Board Statement: Not applicable.

Informed Consent Statement: Not applicable.

Data Availability Statement: Not applicable.

Conflicts of Interest: The authors declare no conflict of interest.

References

1. Liu, X.; Zhai, Y.; Li, S.; Wang, B.; Wang, T.; Liu, Y.; Qiu, Z.; Li, C. Hydrothermal carbonization of sewage sludge: Effect of feed-water pH on hydrochar's physicochemical properties, organic component and thermal behavior. *J. Hazard. Mater.* **2020**, *388*, 122084. [[CrossRef](#)] [[PubMed](#)]
2. Abdel Daiem, M.M.; Said, N.; Negm, A.M. Potential energy from residual biomass of rice straw and sewage sludge in Egypt. *Procedia Manuf.* **2018**, *22*, 818–825. [[CrossRef](#)]
3. Esteban-Gutiérrez, M.; Garcia-Aguirre, J.; Irizar, I.; Aymerich, E. From sewage sludge and agri-food waste to VFA: Individual acid production potential and up-scaling. *Waste Manag.* **2018**, *77*, 203–212. [[CrossRef](#)]
4. Ruqing, N.; Fengyuan, H.; Yunfei, J.; Xinjing, T. Cycle and Harm of Main Pollutants in Thermal System of Gas Turbiner. *IOP Conf. Ser. Earth Environ. Sci.* **2020**, *546*, 32028. [[CrossRef](#)]
5. Li, Y.; Liu, C.; He, F.; Wang, F. Analysis on Water Wall Tube Explosion in a Power Plant. *IOP Conf. Ser. Earth Environ. Sci.* **2020**, *526*, 12162. [[CrossRef](#)]
6. Muncan, J.; Tei, K.; Tsenkova, R. Real-Time Monitoring of Yogurt Fermentation Process by Aquaphotomics Near-Infrared Spectroscopy. *Sensors* **2020**, *21*, 177. [[CrossRef](#)]
7. Jiang, J.; Sun, Y.F.; Tang, X.; He, C.N.; Shao, Y.L.; Tang, Y.J.; Zhou, W.W. Alkaline pH shock enhanced production of validamycin A in fermentation of *Streptomyces hygroscopicus*. *Bioresour. Technol.* **2018**, *249*, 234–240. [[CrossRef](#)]
8. Grzelak, J.; Ąszlęzak, R.; Krzystek, L.; Ledakowicz, S. Effect of pH on the production of volatile fatty acids in dark fermentation process of organic waste. *Ecol. Chem. Eng. S* **2018**, *25*, 295–306. [[CrossRef](#)]

9. Nunes Filho, R.C.; Galvan, D.; Effting, L.; Terhaag, M.M.; Yamashita, F.; Benassi, M.d.T.; Spinosa, W.A. Effects of adding spices with antioxidants compounds in red ale style craft beer: A simplex-centroid mixture design approach. *Food Chem.* **2021**, *365*, 130478. [[CrossRef](#)]
10. Lehnhardt, F.; Nobis, A.; Skornia, A.; Becker, T.; Gastl, M. A Comprehensive Evaluation of Flavor Instability of Beer (Part 1): Influence of Release of Bound State Aldehydes. *Foods* **2021**, *10*, 2432. [[CrossRef](#)]
11. Guimarães, B.P.; Neves, L.E.P.; Guimarães, M.G.; Ghesti, G.F. Evaluation of maturation congeners in beer aged with Brazilian woods. *J. Brew. Distill.* **2020**, *9*, 1–7. [[CrossRef](#)]
12. Nakazawa, N.; Wada, R.; Fukushima, H.; Tanaka, R.; Kono, S.; Okazaki, E. Effect of long-term storage, ultra-low temperature, and freshness on the quality characteristics of frozen tuna meat. *Int. J. Refrig.* **2020**, *112*, 270–280. [[CrossRef](#)]
13. Ezati, P.; Bang, Y.J.; Rhim, J.W. Preparation of a shikonin-based pH-sensitive color indicator for monitoring the freshness of fish and pork. *Food Chem.* **2021**, *337*, 127995. [[CrossRef](#)] [[PubMed](#)]
14. Ezati, P.; Priyadarshi, R.; Bang, Y.J.; Rhim, J.W. CMC and CNF-based intelligent pH-responsive color indicator films integrated with shikonin to monitor fish freshness. *Food Control* **2021**, *126*, 108046. [[CrossRef](#)]
15. Ezati, P.; Tajik, H.; Moradi, M.; Molaei, R. Intelligent pH-sensitive indicator based on starch-cellulose and alizarin dye to track freshness of rainbow trout fillet. *Int. J. Biol. Macromol.* **2019**, *132*, 157–165. [[CrossRef](#)]
16. Ogunniyi, A.D.; Tenzin, S.; Ferro, S.; Venter, H.; Pi, H.; Amorico, T.; Deo, P.; Trott, D.J. A pH-neutral electrolyzed oxidizing water significantly reduces microbial contamination of fresh spinach leaves. *Food Microbiol.* **2021**, *93*, 103614. [[CrossRef](#)]
17. Ding, Z.; Johanningsmeier, S.D.; Price, R.; Reynolds, R.; Truong, V.D.; Payton, S.C.; Breidt, F. Evaluation of nitrate and nitrite contents in pickled fruit and vegetable products. *Food Control* **2018**, *90*, 304–311. [[CrossRef](#)]
18. Alegbeleye, O.O.; Singleton, I.; Sant’Ana, A.S. Sources and contamination routes of microbial pathogens to fresh produce during field cultivation: A review. *Food Microbiol.* **2018**, *73*, 177–208. [[CrossRef](#)]
19. Kassim, M.R.M. IoT Applications in Smart Agriculture: Issues and Challenges. In Proceedings of the 2020 IEEE Conference on Open Systems (ICOS), Kota Kinabalu, Malaysia, 17–19 November 2020; pp. 19–24. [[CrossRef](#)]
20. Jürkenbeck, K.; Heumann, A.; Spiller, A. Sustainability Matters: Consumer Acceptance of Different Vertical Farming Systems. *Sustainability* **2019**, *11*, 4052. [[CrossRef](#)]
21. Al-Kodmany, K. The Vertical Farm: A Review of Developments and Implications for the Vertical City. *Buildings* **2018**, *8*, 24. [[CrossRef](#)]
22. Dagar, R.; Som, S.; Khatri, S.K. Smart Farming—IoT in Agriculture. In Proceedings of the 2018 International Conference on Inventive Research in Computing Applications (ICIRCA), Coimbatore, India, 11–12 July 2018; pp. 1052–1056. [[CrossRef](#)]
23. Penn, C.J.; Camberato, J.J. A Critical Review on Soil Chemical Processes that Control How Soil pH Affects Phosphorus Availability to Plants. *Agriculture* **2019**, *9*, 120. [[CrossRef](#)]
24. Jin, H.; Qin, Y.; Pan, S.; Alam, A.U.; Dong, S.; Ghosh, R.; Deen, M.J. Open-Source Low-Cost Wireless Potentiometric Instrument for pH Determination Experiments. *J. Chem. Educ.* **2018**, *95*, 326–330. [[CrossRef](#)]
25. Inserra, B.; Hayashi, K.; Marchisio, A.; Tulliani, J.M. Sol-gel-entrapped pH indicator for monitoring pH variations in cementitious materials. *J. Appl. Biomater. Funct. Mater.* **2020**, *18*, 2280800020936540. [[CrossRef](#)] [[PubMed](#)]
26. Ghoneim, M.T.; Nguyen, A.; Dereje, N.; Huang, J.; Moore, G.C.; Murzynowski, P.J.; Dagdeviren, C. Recent Progress in Electrochemical pH-Sensing Materials and Configurations for Biomedical Applications. *Chem. Rev.* **2019**, *119*, 5248–5297. [[CrossRef](#)] [[PubMed](#)]
27. Yoon, J.H.; Kim, S.M.; Park, H.J.; Kim, Y.K.; Oh, D.X.; Cho, H.W.; Lee, K.G.; Hwang, S.Y.; Park, J.; Choi, B.G. Highly self-healable and flexible cable-type pH sensors for real-time monitoring of human fluids. *Biosens. Bioelectron.* **2020**, *150*, 111946. [[CrossRef](#)] [[PubMed](#)]
28. Manjakkal, L.; Sakthivel, B.; Gopalakrishnan, N.; Dahiya, R. Printed flexible electrochemical pH sensors based on CuO nanorods. *Sens. Actuators B Chem.* **2018**, *263*, 50–58. [[CrossRef](#)]
29. Dang, W.; Manjakkal, L.; Navaraj, W.T.; Lorenzelli, L.; Vinciguerra, V.; Dahiya, R. Stretchable wireless system for sweat pH monitoring. *Biosens. Bioelectron.* **2018**, *107*, 192–202. [[CrossRef](#)]
30. Córdoba, C.; Mera, J.; Paredes, O.; Benavides, J. Sensor óptico para mediciones de PH obtenido por el método sol-gel con moléculas orgánicas dopadas en matriz vítrea. *Rev. Soc. Química México* **2004**, *48*, 203–207.
31. Rasheed, H.S.; Ahmed, N.M.; Matjafri, M.Z. Ag metal mid layer based on new sensing multilayers structure extended gate field effect transistor (EG-FET) for pH sensor. *Mater. Sci. Semicond. Process.* **2018**, *74*, 51–56. [[CrossRef](#)]
32. Sinha, S.; Pal, T.; Kumar, D.; Sharma, R.; Kharbanda, D.; Khanna, P.K.; Mukhiya, R. Design, fabrication and characterization of TiN sensing film-based ISFET pH sensor. *Mater. Lett.* **2021**, *304*, 130556. [[CrossRef](#)]
33. FAO. *El Estado Mundial de la Agricultura y la Alimentación 2021*; Food and Agriculture Organization of the United Nations: Rome, Italy, 2021. [[CrossRef](#)]
34. Kurzweil, P. Metal Oxides and Ion-Exchanging Surfaces as pH Sensors in Liquids: State-of-the-Art and Outlook. *Sensors* **2009**, *9*, 4955–4985. [[CrossRef](#)]
35. Manjakkal, L.; Szwagierczak, D.; Dahiya, R. Metal oxides based electrochemical pH sensors: Current progress and future perspectives. *Prog. Mater. Sci.* **2020**, *109*, 100635. [[CrossRef](#)]
36. Alva, S.; Binti Abdul Aziz, A.S.; Bin Syono, M.I.; Bin Wan Jamil, W.A. Ag/AgCl Reference Electrode Based on Thin Film of Arabic Gum Membrane. *Indones. J. Chem.* **2018**, *18*, 479–485. [[CrossRef](#)]

37. Westbroek, P. Electrochemical methods. *Anal. Electrochem. Text.* **2005**, 37–69. [[CrossRef](#)]
38. Levanov, A.V.; Isaikina, O.Y.; Lunin, V.V. Determining the Potential of a Silver/Silver Chloride Electrode at Different Temperatures. *Russ. J. Phys. Chem. A* **2019**, *93*, 770–773. [[CrossRef](#)]
39. Lonsetta, A.M.; Cope, P.; Campbell, J.; Mohd, B.J.; Hayajneh, T. Actuator Networks Sensor and Security Vulnerabilities in Bluetooth Technology as Used in IoT. *J. Sens. Actuator Netw.* **2018**, *7*, 28. [[CrossRef](#)]
40. Ghorri, M.R.; Wan, T.-C.; Sodhy, G.C. Bluetooth Low Energy Mesh Networks: Survey of Communication and Security Protocols. *Sensors* **2020**, *20*, 3590. [[CrossRef](#)]
41. Shylendra, S.P.; Lonsdale, W.; Wajrak, M.; Nur-e-alam, M.; Alameh, K. Titanium Nitride Thin Film Based Low-Redox-Interference Potentiometric pH Sensing Electrodes. *Sensors* **2020**, *21*, 42. [[CrossRef](#)]
42. Sharma, N.; Acharya, S.; Kumar, K.; Singh, N.; Chaurasia, O.P. Hydroponics as an advanced technique for vegetable production: An overview. *J. Soil Water Conserv.* **2018**, *17*, 364–371. [[CrossRef](#)]
43. Montes Rivera, M.; Escalante-Garcia, N.; Dena-Aguilar, J.A.; Olvera-Gonzalez, E.; Vacas-Jacques, P. Feature Selection to Predict LED Light Energy Consumption with Specific Light Recipes in Closed Plant Production Systems. *Appl. Sci.* **2022**, *12*, 5901. [[CrossRef](#)]
44. Olvera-Gonzalez, E.; Montes Rivera, M.; Escalante-Garcia, N.; Flores-Gallegos, E. Modeling Energy LED Light Consumption Based on an Artificial Intelligent Method Applied to Closed Plant Production System. *Appl. Sci.* **2021**, *11*, 2735. [[CrossRef](#)]